THE JOURNAL OF BIOLOGICAL CHEMISTRY VOL. 282, NO. 9, pp. 6136–6142, March 2, 2007

Biochemical Characterization of a Regulatory Cascade Controlling Transcription of the *Pseudomonas aeruginosa* Type III Secretion System*

Received for publication, December 20, 2006 Published, JBC Papers in Press, December 29, 2006, DOI 10.1074/jbc.M611664200

Zhida Zheng[‡], Guozhou Chen[‡], Shreyas Joshi[‡], Evan D. Brutinel[§], Timothy L. Yahr[§], and Lingling Chen[‡¶1]

From the [‡]Department of Biology and the [¶]Interdisciplinary Biochemistry Program, Indiana University, Bloomington, Indiana 47405 and the [§]Department of Microbiology, University of Iowa, Iowa City, Iowa 52242

Many Gram-negative pathogens utilize type III secretion systems (T3SS) to translocate effector proteins into eukaryotic host cells. Expression of T3SS genes is highly regulated and is often coupled to type III secretory activity. Transcription of the *Pseudomonas aeruginosa* T3SS genes is coupled to secretion by a cascade of interacting regulatory proteins (ExsA, ExsD, ExsC, and ExsE). ExsA is an activator of type III gene transcription, ExsD binds ExsA to inhibit transcription, ExsC inhibits ExsD activity, and ExsE inhibits ExsC activity. The entire process is coupled to secretion by virtue of the fact that ExsE is a secreted substrate of the T3SS. Changes in the intracellular concentration of ExsE are thought to govern formation of the ExsC-ExsE, ExsC-ExsD, and ExsD-ExsA complexes. Whereas formation of the ExsC-ExsE complex allows ExsD to bind ExsA and transcription of the T3SS is repressed, formation of the ExsC-ExsD complex sequesters ExsD from ExsA and transcription of the T3SS is induced. In this study, we characterized the self-association states of ExsC, ExsD, and ExsE and the binding interactions of ExsC with ExsE and ExsD. ExsC exists as a homodimer and binds one molecule of ExsE substrate. Dimeric ExsC also interacts directly with ExsD to form a heterotetrameric complex. The difference in binding affinities between the ExsC-ExsE (K_d 1 nM) and ExsC-ExsD (K_d 18 nM) complexes supports a model in which ExsC preferentially binds cytoplasmic ExsE, resulting in the inhibition of T3SS gene transcription.

Pseudomonas aeruginosa is a Gram-negative opportunistic pathogen and a primary cause of pneumonia and urinary tract infections in intensive care units (1, 2). Among the most vulnerable individuals are those with immunodeficiency, cystic fibrosis, or severe burns or who require mechanical ventilation. A major virulence determinant of *P. aeruginosa* is a type III secretion system (T3SS).[2] The T3SS encodes a multiprotein complex, called an injectisome, which functions by injecting or translocating effector proteins directly into the cytoplasm of eukaryotic host cells. The T3SS of *P. aeruginosa* is used to translocate four known effectors that subvert signal transduction pathways to inhibit phagocytosis and elicit cytotoxicity toward host cells (3, 4).

Expression of the *P. aeruginosa* T3SS is highly regulated and under the direct transcriptional control of ExsA, a member of the AraC family of transcriptional activators (5). Environmental signals, including contact of *P. aeruginosa* with host cells and Ca^{2+}-limiting growth conditions, induce ExsA-dependent transcription of the T3SS (6, 7). Although the mechanism of induction by host cell contact is unclear, Ca^{2+} depletion regulates T3SS gene transcription by inducing type III secretory activity (8). Transcription of T3SS genes is intimately coupled to type III secretory activity through a regulatory cascade that governs ExsA activity. This regulatory cascade consists of three interacting proteins (ExsD, ExsC, and ExsE). ExsD functions as an anti-activator by directly binding to and inhibiting ExsA-dependent transcription (8). ExsC functions as an anti-anti-activator by binding to and antagonizing ExsD activity (9). Finally, ExsE is an inhibitor of ExsC activity and a secreted substrate of the T3SS (10, 11). Dasgupta *et al.* (9) have proposed the following model to account for transcriptional induction of T3SS genes by Ca^{2+} depletion. Under Ca^{2+} replete conditions, ExsE is retained in the cytoplasm because of the lack of type III secretory activity and forms a complex with ExsC. The sequestration of ExsC by ExsE allows for the binding of the anti-activator ExsD to ExsA, thereby blocking transcription. In response to Ca^{2+} depletion, however, ExsE is secreted into the extracellular milieu. The corresponding decrease in intracellular ExsE levels releases ExsC, which then sequesters ExsD and thereby makes ExsA available to activate transcription of T3SS genes.

A common feature of proteins secreted by the T3SS is the requirement for chaperone activity (12). ExsC has biochemical characteristics of a type III-specific chaperone and is required for ExsE stability within the cytoplasm and for ExsE secretion (9, 10). T3SS-specific chaperones fall into one of three classes based on substrate specificity. Class I, II, and III chaperones facilitate secretion of effectors, components of the transloca-

* This work was supported by grants from the Howard Hughes Medical Institute Biomedical Research Support Faculty Start-up Program (to T. L. Y.) and the University of Iowa W. M. Keck Microbial Communities and Cell Signaling Program (to T. L. Y.), National Institutes of Health Grants R01-AI055042 (to T. L. Y.) and R01-GM065260-01A1 (to L. C.), and National Science Foundation Grant MCB-0416447 (to L. C.). The costs of publication of this article were defrayed in part by the payment of page charges. This article must therefore be hereby marked "*advertisement*" in accordance with 18 U.S.C. Section 1734 solely to indicate this fact.

[1] To whom correspondence should be addressed: Dept. of Biology, 915 E. 3rd St., Indiana University, Bloomington, IN 47405. Tel.: 812-855-0491; Fax: 812-855-6082; E-mail: linchen@indiana.edu.

[2] The abbreviations used are: T3SS, type III secretion system; Tev, tobacco etch virus; AUC, analytical ultracentrifugation; ITC, isothermal titration calorimetry.

tion channel, and components of the injectisome, respectively (13). Members of the Class I family are generally small in size (100–150 amino acids), acidic, and usually encoded adjacent to their cognate effector gene. Based on these characteristics, ExsC is likely a member of the class I chaperone family. The solved three-dimensional structures of several class I chaperones reveals a dimeric binding configuration with each monomer possessing a conserved fold consisting of five β-strands and three α-helices. Although the precise role of the T3SS chaperones is unclear, proposed functions include targeting of substrates to the secretion machinery, maintaining substrates in a secretion competent conformation, preventing substrate aggregation prior to secretion, and establishing a secretion hierarchy among different substrates (12). In the case of ExsC, the primary role appears to be protection of ExsE from proteolysis in the cytoplasm (10).

In addition to the role in secretion, many type III-specific chaperones are also involved in transcriptional regulation of T3SS gene expression (14–16). ExsC functions as an anti-anti-activator by sequestering the ExsD anti-activator (9). A recent study found that purified ExsC and ExsD individually form self-associated oligomeric complexes as judged by gel filtration chromatography (17). In addition, incubation of purified ExsC with ExsD resulted in the formation of a large molecular weight complex. Neither the subunit composition of the self-associated ExsC or ExsD complexes nor the binding stoichiometry of the ExsC-ExsD complex, however, could be accurately determined by gel filtration.

In the present study the oligomeric states of ExsE, ExsC, ExsD, as well as the complexes of ExsC-ExsD and ExsC-ExsE were characterized by analytical ultracentrifugation. By this technique purified ExsE exists as monomers, ExsC forms homodimers, and ExsD self-associates into homotrimers. In addition, the subunit stoichiometry of the ExsC-ExsD and ExsC-ExsE complexes was resolved to 2:2 and 2:1, respectively. Thus, it appears that the trimeric ExsD dissociates in forming the heterotetrameric ExsC-ExsD complex, whereas the dimeric ExsC maintains during complex formation. The binding affinities for the ExsC-ExsD and ExsC-ExsE complexes were studied by isothermal calorimetry. The tighter interaction of the ExsC-ExsE (1 nM) complex when compared with the ExsC-ExsD (18 nM) complex is supportive of a model in which preferential binding of ExsC to ExsE results in inhibition of T3SS gene expression in the absence of type III secretory activity.

EXPERIMENTAL PROCEDURES

Protein Expression and Purification—The genes encoding ExsC and ExsD were amplified by PCR and individually cloned into pET25b (Novagen) with NdeI/XhoI restriction sites resulting in carboxyl-terminal histidine-tagged (LEIKRASQPELAPEDPEDVEHHHHHH, 3088 Da) fusion proteins (termed $ExsC_{His6}$ and $ExsD_{His6}$). *exsC* with a Tev protease site before the carboxyl-terminal hexahistidine tag was also cloned into pET24a (Novagen) using NdeI/XhoI restriction sites (termed $ExsC_{Tev\text{-}His6}$). For the ExsC-ExsD and ExsC-ExsE co-expression studies, the genes were cloned into the pCOLADuet-1 (Novagen) expression vector. The gene encoding ExsC was PCR-amplified and cloned as an NcoI/NotI restriction fragment into the corresponding sites of MCS1 in pCOLADuet-1. ExsC expressed from this vector ($ExsC_{His6\text{-}short}$) carries a carboxyl-terminal hexahistidine tag (LEHHHHHH, 1083 Da) encoded by the PCR primer. The genes encoding ExsD and ExsE were cloned into MSC2 as NdeI/XhoI restriction fragments.

Proteins were expressed in *Escherichia coli* BL21(DE3) codon-plus (Novagen) grown in LB medium at 37 °C to an optical density at 600 nm (A_{600}) of 0.6. The growth temperature was reduced to 23 °C before induction with 0.1 mM isopropyl 1-thio-β-D-galactopyranoside, and cell growth continued for 5–8 h. Cells were lysed at 4 °C in 50 mM sodium phosphate (pH 8.0), 300 mM NaCl, and 5 mM imidazole using a continuous flow microfluidizer (Microfluidics). The soluble fraction was loaded onto a Ni^{2+} chelating column (Amersham Biosciences), and bound protein was eluted over a linear imidazole gradient (5 mM to 500 mM) in 50 mM sodium phosphate (pH 8.0) and 300 mM NaCl. Protein fractions were combined, concentrated by Centriprep YM10 (Millipore), dialyzed against 50 mM imidazole (pH 7.0), 100 mM NaCl, 0.5 mM EDTA, and 1 mM β-mercaptoethanol, and loaded onto a FastQ column (Amersham Biosciences). The protein was eluted over a linear NaCl gradient (100–1000 mM) in 50 mM imidazole (pH 7.0), 0.5 mM EDTA, and 1 mM β-mercaptoethanol. Peak protein fractions were concentrated by Centriprep YM10 (Millipore), dialyzed against buffer (50 mM imidazole (pH 7.0), 200 mM NaCl, 0.5 mM EDTA, and 1 mM β-mercaptoethanol), and loaded onto a Superdex 200 gel filtration column (Amersham Biosciences). The purified protein was assessed by SDS-PAGE to be at least 95% pure.

To obtain the native form of ExsC, purified $ExsC_{Tev\text{-}His6}$ was incubated with His_6-tagged Tev protease at 4 °C for 72 h. The mixture was passed through Ni^{2+} chelating resin (Amersham Biosciences) to remove the digested His6-tag, the undigested $ExsC_{Tev\text{-}His6}$, and the Tev protease. The unbound material was loaded onto a Superdex 200 gel filtration column for further purification. The native form of ExsD was generated as follows. Purified $ExsC_{His6\text{-}short}$-ExsD complex was incubated with an excess amount of purified $ExsE_C$ (defined below) at 4 °C for 24 h, and the reaction mixture was loaded on a Ni^{2+} cheating column to remove $ExsC_{His6\text{-}short}$-ExsE and the residual $ExsC_{His6\text{-}short}$-ExsD. The unbound fraction was further purified by gel filtration via a Superdex 200 column.

The gene encoding ExsE was PCR-amplified and cloned into pTWIN1 (New England Biolabs) as an NdeI/EcoRI restriction fragment resulting in an ExsE-chitin-binding fusion protein separated by an Mxe intein. Following cleavage of the intein, seven amino acid residues (EFLEGSS, 768 Da) remain at the carboxyl terminus of ExsE (designated $ExsE_C$). Expression of $ExsE_C$ was induced with 0.4 mM isopropyl 1-thio-β-D-galactopyranoside for 4 h at 37 °C. Cells were lysed in buffer A (20 mM Tris-Cl (pH 7.0), 500 mM NaCl, and 1 mM EDTA), and the cleared lysate was loaded onto a chitin column (New England Biolabs). The column was washed extensively with buffer A and then incubated with buffer B (buffer A plus 40 mM dithiothreitol (pH 8.5)) overnight at 4 °C to remove the intein fusion partner from ExsE. $ExsE_C$ was further purified using a Superdex 75 column (Amersham Biosciences).

Analytical Ultracentrifugation (AUC)—Equilibrium sedimentation experiments were carried out at 25 °C using a Beckman XL-A Ultracentrifuge with an AN-Ti-60 rotor. The buffer for all the AUC experiments contained 50 mM sodium phosphate (pH 7.0), 200 mM NaCl, and 0.5 mM EDTA. Data were collected at three protein concentrations and with different rotor speeds optimized according to the expected molecular weight: $ExsC_{His6}$ (0.75, 0.37, 0.19 mg/ml; 7900, 9500, 12,000, 14,000, 18,000 rpm); $ExsD_{His6}$ (0.2, 0.1, 0.05 mg/ml; 6500, 7800, 11,500 rpm); $ExsE_C$ (1.2, 0.86, 0.51 mg/ml; 13,000, 16,000, 23,000 rpm); $ExsC_{His6\text{-}short}$-ExsE (0.75, 0.38, 0.19 mg/ml; 9000, 11,000, 16,000 rpm); $ExsC_{His6}$-$ExsD_{His6}$ (0.3, 0.15, 0.075 mg/ml; 6000, 7500, 10,500 rpm); $ExsC_{His6}$-$ExsE_C$ (0.77, 0.38, 0.19 mg/ml; 8300, 10,000, 14,500 rpm). The scanning wavelength was 280 nm. The partial specific volume of each protein or protein complex was calculated from the amino acid sequence: $ExsC_{His6}$ (0.732 $cm^3\ g^{-1}$), $ExsD_{His6}$ (0.723 $cm^3\ g^{-1}$), $ExsE_C$ (0.711 $cm^3\ g^{-1}$), $ExsC_{His6}$-$ExsD_{His6}$ (0.727 $cm^3\ g^{-1}$), $ExsC_{His6\text{-}short}$-ExsE (0.723 $cm^3\ g^{-1}$), and $ExsC_{His6}$-ExsEc (0.7279 $cm^3\ g^{-1}$).

Isothermal Titration Calorimetry (ITC)—ITC experiments were carried at 25 °C using a VP-ITC instrument (MicroCal). Protein samples were dialyzed overnight to a buffer containing 50 mM sodium phosphate (pH 7.5), 200 mM NaCl, 0.5 mM EDTA. Two experiments were performed for each study. For example, to study the interaction between $ExsC_{His6}$ and $ExsD_{His6}$, 30 injections of 10 μl of $ExsC_{His6}$ (150 μM) were titrated to 1.4 ml of $ExsD_{His6}$ (15 μM). A second experiment was done by reversing the injectant and the titratant: 30 injections of $ExsD_{His6}$ (110 μM) into 1.4 ml of $ExsC_{His6}$ (10 μM). Thermodynamic parameters of the binding process were derived using ORIGIN ITC software (OriginLab) by fitting the corrected binding isotherm to a single-site binding model.

RESULTS

Protein Expression and Purification—To characterize the oligomeric state and binding interactions of ExsC, ExsE, and ExsD, each of the proteins was individually expressed in *E. coli*. ExsC and ExsD were expressed as carboxyl-terminally tagged hexahistidine fusion proteins ($ExsC_{His6}$ and $ExsD_{His6}$) and sequentially purified by Ni^{2+} affinity, ion exchange, and gel filtration chromatography. ExsE was expressed as a chitin-binding domain fusion separated by an intein and purified by chitin affinity chromatography. Following intein cleavage and removal of the chitin binding domain, ExsE contained an additional seven amino acids at the carboxyl terminus ($ExsE_C$). $ExsE_C$ was further purified by gel filtration chromatography (Fig. 1*A*). Each of the purified proteins was judged by SDS-PAGE to be >95% pure (Fig. 1*B*). Complexes of ExsC-ExsD and ExsC-ExsE were formed by incubating $ExsD_{His6}$ with a 2-fold molar excess of purified $ExsC_{His6}$ or $ExsC_{His6}$ with a 2-fold molar excess of $ExsE_C$, respectively, and purified by gel filtration chromatography (Fig. 1*A*). The presence of individual components within each complex was verified by SDS-PAGE (Fig. 1*B*).

Oligomeric State of ExsC, ExsD, and ExsE—The respective molecular mass sizes of monomeric $ExsC_{His6}$ and $ExsD_{His6}$ are 19.342 and 33.941 kDa as determined by mass spectrometry. A previous study found that purified $ExsC_{His6}$ and $ExsD_{His6}$ migrate as 79- and 128-kDa molecular species, respectively, as determined by gel filtration chromatography (Fig. 1*A*) (17). These findings indicated that purified ExsC and ExsD form self-associated oligomeric complexes, potentially tetrameric in state. To further assess the molecular weight of the self-associated complexes, we employed AUC. Using this technique the molecular weights of the $ExsC_{His6}$ and $ExsD_{His6}$ self-associated complexes was determined to be 47.2 ± 2.0 and 101.1 ± 1.6 kDa, respectively. These data suggest that $ExsC_{His6}$ exists as a dimer, whereas $ExsD_{His6}$ exists as a trimer. We also carried out AUC experiments on purified untagged ExsD (native form) and derived its molecular weight to be 96.6 ± 1.7 kDa, consistent

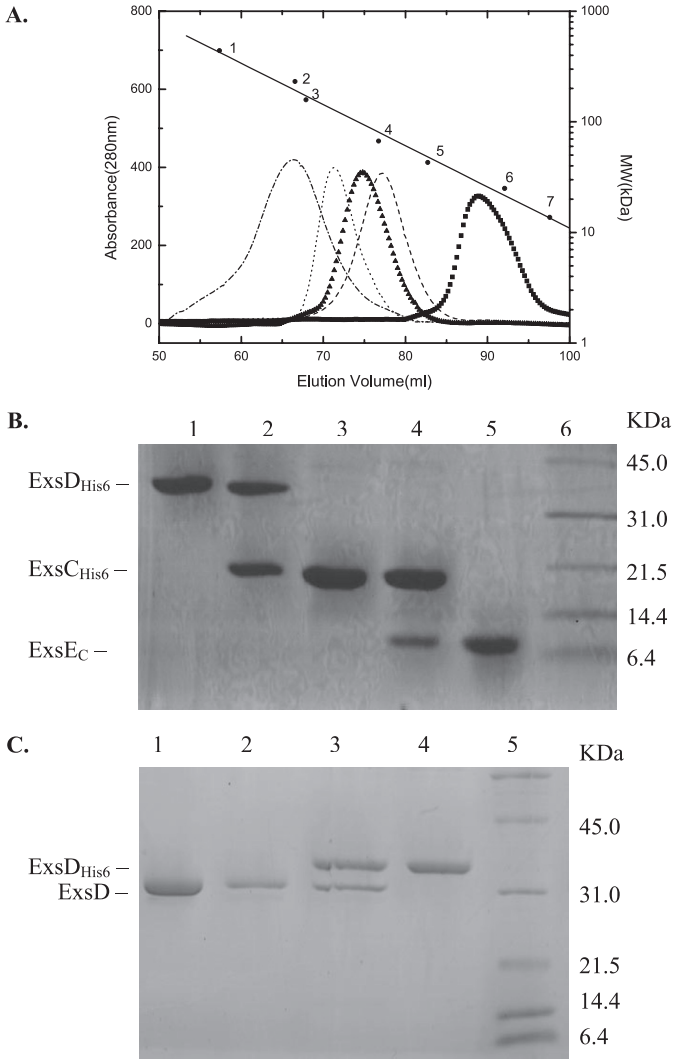

FIGURE 1. *A*, gel filtration profiles of $ExsE_C$ (■), $ExsC_{His6}$-$ExsE_C$ (▲), $ExsC_{His6}$ (*dashed line*), $ExsD_{His6}$ (*dotted line*), and $ExsC_{His6}$-$ExsD_{His6}$ (*dashed-dotted line*). Also shown are the elution volumes of protein calibration standards with known molecular mass sizes: *1*, ferritin, 440 kDa; *2*, catalase, 232 kDa; *3*, aldolase, 158 kDa; *4*, albumin, 67 kDa; *5*, ovalbumin, 43 kDa; *6*, chymotrypsinogen A, 25 kDa; *7*, ribonuclease A, 13.7 kDa. *B*, Coomassie-stained SDS-polyacrylamide gel showing purified $ExsD_{His6}$ (*lane 1*), $ExsC_{His6}$-$ExsD_{His6}$ complex (*lane 2*), $ExsC_{His6}$ (*lane 3*), $ExsC_{His6}$-$ExsE_C$ complex (*lane 4*), and $ExsE_C$ (*lane 5*). Molecular mass standards are shown on the *right-hand side* of the gel. *C*, mixture of $ExsD_{His6}$ with untagged ExsD over the Ni^{2+} chelating column on an imidazole gradient. *Lanes 1* and *4*, control samples of ExsD and $ExsD_{His6}$, respectively, over 24 h; *lane 2*, the unbound fraction; *lane 3*, the fraction corresponding to the elution peak; *lane 5*, molecular mass standards.

with a homotrimeric state (predicted molecular mass = 97.3 kDa). Thus, the presence of the carboxyl-terminal His tag (3.1 kDa) did not affect the aggregation state of ExsD.

The molecular weight of monomeric $ExsE_C$ is 9.422 kDa by mass spectrometry. Whereas $ExsE_C$ migrated as a 28-kDa molecular species by gel filtration (Fig. 1*A*), its molecular mass was found to be 9.5 ± 0.5 kDa by AUC, indicating that $ExsE_C$ exists in a monomeric state. For all three proteins, the larger molecular mass as estimated by gel filtration compared with that by AUC is indicative of an asymmetric molecular shape (18).

Stability of the Oligomeric State of ExsC and ExsD—To examine monomer interactions within the ExsD complex, mixture of $ExsD_{His6}$ and ExsD (1:1 molar ratio) as well as the individual $ExsD_{His6}$ and ExsD were kept at 4 °C for 24 h. The mixture was loaded onto a Ni^{2+} chelating column. Following extensive washing, bound protein was eluted over an imidazole gradient, and fractions corresponding to the elution peaks were concentrated and analyzed by SDS-PAGE. Because trimeric ExsD does not bind to the Ni^{2+} resin (see "Experimental Procedure"), it eluted as the unbound portion (Fig. 1*C*, *lane 2*). Nevertheless, a substantial amount of ExsD was also found in the fraction corresponding to the elution peak (Fig. 1*C*, *lane 3*). Presumably, this "bound" ExsD might be retained by the Ni^{2+} resin in forms of $(ExsD_{His6})_n(ExsD)_{3-n}$ (n = 1 or 2). These data suggest that trimeric ExsD may dissociate into smaller oligomeric states (monomer and dimer) and reassemble to generate mixed trimeric species. A similar experiment was carried out using $ExsC_{His6}$ and native ExsC. In contrast to ExsD, native ExsC was not present in the elution fractions from the Ni^{2+} chelating column (data not shown). Taken together, it appears that the subunit assembly in trimeric ExsD is dynamic, whereas the monomer associations within dimeric ExsC are much stronger.

Molecular Masses of the ExsC-ExsD and ExsC-ExsE Complexes—A previous study found that purified $ExsC_{His6}$ and $ExsD_{His6}$ readily formed a complex when co-incubated for 16 h at 4 °C (17). The isolated $ExsC_{His6}$-$ExsD_{His6}$ complex migrates with an apparent molecular mass of 197 kDa by gel filtration chromatography (Fig. 1*A*). Analysis of the same complex by AUC, however, yielded a much smaller molecular mass of 100.1 ± 1.6 kDa (Fig. 2*A*). The AUC data are indicative of a complex consisting of two molecules of both $ExsC_{His6}$ and $ExsD_{His6}$ (which has a predicted molecular mass of 106.6 kDa). This conclusion is further supported by previous ITC data, which predicted an equal molar binding ratio of ExsC and ExsD within the complex (n = 0.87) (17).

Similar to the experiments described above, incubation of purified $ExsC_{His6}$ with a molar excess of $ExsE_C$ resulted in the formation of an $ExsC_{His6}$-$ExsE_C$ complex. The complex isolated by gel filtration chromatography migrated as a 96.1-kDa species (Fig. 1*A*), and the presence of both $ExsC_{His6}$ and $ExsE_C$ were verified by SDS-PAGE (Fig. 1*B*). By AUC, however, the molecular mass of the $ExsC_{His6}$-$ExsE_C$ complex was determined to be 46.9 ± 1.2 kDa (Fig. 2*B*). The ExsC-ExsE complex was also isolated by co-expressing $ExsC_{His6\text{-}short}$ and native ExsE in *E. coli* and subsequent purification by Ni^{2+} affinity chromatography. This purified $ExsC_{His6\text{-}short}$-ExsE complex migrates as a 63.4-kDa species by gel filtration, and its molecular mass was determined by AUC to be 45.7 ± 1.0 kDa. Both molecular masses derived from AUC are consistent with a complex containing dimeric ExsC bound to one ExsE monomer (predicted molecular mass values: 48.1 kDa for $ExsC_{His6}$-$ExsE_C$ and 43.7 kDa for $ExsC_{His6\text{-}short}$-ExsE).

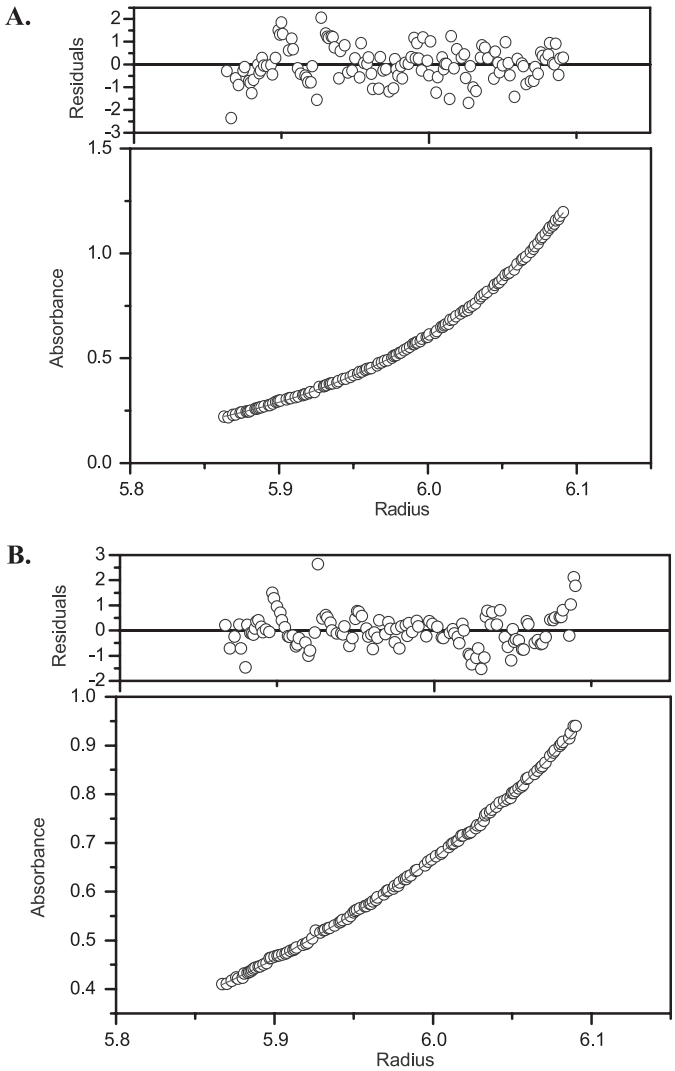

FIGURE 2. **Sedimentation equilibrium analyses of the $ExsC_{His6}$-$ExsD_{His6}$ complex (*A*) and the $ExsC_{His6}$-$ExsE_C$ complex (*B*).** The experimental conditions are described under "Experimental Procedures." Nine data sets were simultaneously fitted into a single species model; the data fitting is shown in the *lower panels* and the fitting residual in the *upper panels*.

Binding Stoichiometry of ExsC-ExsE Complex—Formation of the ExsC-ExsE complex was further examined by mixing purified $ExsC_{His6}$ and $ExsE_C$ in various molar ratios (1:0.5, 1:1, 1:2, and 1:4) and incubating them for 16 h at 4 °C. At molar ratios greater than 1:0.5, an excess of $ExsE_C$ was detected by gel filtration chromatography, suggesting that $ExsC_{His6}$ binds $ExsE_C$ in a 1:0.5 (or 2:1) molar ratio (Fig. 3*A*). This binding stoichiometry was further confirmed by ITC, where the binding ratio was determined to be 2.08 (Fig. *3B*). These results, combined with the AUC data, are consistent with a complex consisting of one $ExsC_{His6}$ dimer bound to one monomer of $ExsE_C$.

Binding Affinity of ExsC for ExsD and ExsE—A previous study employing ITC found formation of the $(ExsC_{His6})_2$·$(ExsD_{His6})_2$ complex to be exothermic and energetically favorable, with a

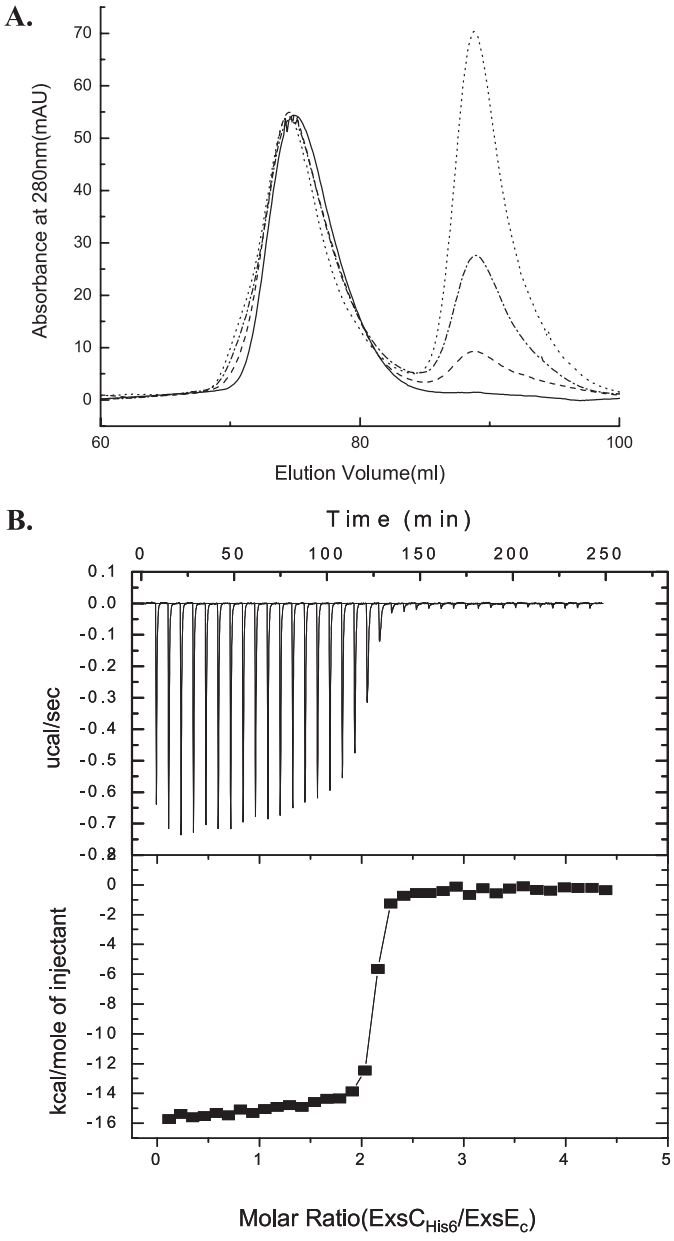

FIGURE 3. *A*, binding ratio within the ExsC-ExsE complex. $ExsC_{His6}$ and $ExsE_C$ were incubated at various molar ratios (1:0.5, *solid line*; 1:1, *dashed line;* 1:2, *dashed-dotted line*; 1:4, *dotted line*) in 50 mM imidazole (pH 7.0), 200 mM NaCl, 0.5 mM EDTA, and 0.5 mM β-mercaptoethanol, and the mixture was applied to a Superdex 200 gel filtration column. The chromatograms are normalized to the amount of $ExsE_C$ input. The first elution peak, centered at 74.6 ml, is the $ExsC_{His6}$-$ExsE_C$ complex as it resolves into $ExsC_{His6}$ and $ExsE_C$ by SDS-PAGE; the second peak, centered at 88.8 ml, corresponds to isolated $ExsE_C$ as confirmed by SDS-PAGE. *B*, ITC data for the interaction of $ExsC_{His6}$ and $ExsE_C$. Shown here is the titration of $ExsC_{His6}$ into $ExsE_C$. The *upper panel* shows the heat exchange during each injection, and the *lower panel* shows the corresponding integrated enthalpies (after background correction).

dissociation constant (K_d) of 18 nM and an enthalpy release (ΔH) of 7.6 kcal/mol (17). Using the same method, the K_d and ΔH of the $(ExsC_{His6})_2$·$ExsE_C$ complex were found to 1 nM and 31.5 kcal/mol, respectively (Fig. 3*B*), indicating that ExsC has a stronger binding affinity for ExsE when compared with ExsD.

Three experiments were conducted to confirm that ExsC has a high binding affinity for ExsE. In the first experiment, samples of $ExsC_{His6}$, $ExsD_{His6}$, and $ExsE_C$ were co-incubated at a molar ratio of 1:1:0.5, respectively, and incubated at 4 °C for 16 h. Analysis of the mixture by gel filtration revealed a single peak (Fig. 4*A*). Because the elution profiles of the $(ExsC_{His6})_2$·$ExsE_C$ complex and the $ExsD_{His6}$ self-associated complex demonstrate significant overlap (Fig. 1*A*), fractions corresponding to the leading shoulder (fraction 1), peak (fraction 2), and trailing shoulder (fractions 3–4) were subjected to SDS-PAGE and Coomassie staining. Fractions 1 and 2 consist primarily of $ExsD_{His6}$ (which elutes at 71.4 ml), whereas fractions 3 and 4 consist of a mixture of $ExsD_{His6}$ and the $(ExsC_{His6})_2$·$ExsE_C$ complex (which elutes at 74.7 ml). Notably, peaks corresponding to monomeric $ExsE_C$ (which elutes at 88.6 ml) and the $(ExsC_{His6})_2$·$(ExsD_{His6})_2$ complex (which elutes at 66.4 ml) were not detected. These data suggest that all of the $ExsE_C$ exists in a complex with $ExsC_{His6}$ and that $ExsC_{His6}$ does not bind to $ExsD_{His6}$ in the presence of $ExsE_C$.

The second experiment addressed whether $ExsE_C$ could disrupt the preformed $(ExsC_{His6})_2$·$(ExsD_{His6})_2$ complex. $ExsE_C$ was incubated with the purified $(ExsC_{His6})_2$·$(ExsD_{His6})_2$ complex for 16 h at 4 °C, and the mixture was analyzed by gel filtration. Remarkably, peaks corresponding to the input materials, monomeric $ExsE_C$ (88.6 ml) and the $(ExsC_{His6})_2$·$(ExsD_{His6})_2$ complex (66.4 ml), were greatly diminished (Fig. 4*B*). In place of the input materials was a composite elution profile with a peak centered at 72.2 ml, likely resulting from the overlapping elution profiles of $(ExsC_{His6})_2$·$ExsE_C$ and $ExsD_{His6}$. By SDS-PAGE, the leading shoulder (fraction 1) consisted mainly of $ExsD_{His6}$, whereas the trailing shoulder contained $ExsC_{His6}$ and $ExsE_C$ (fraction 4–5) or the $(ExsC_{His6})_2$·$ExsE_C$ complex. These results suggest that the $(ExsC_{His6})_2$·$(ExsD_{His6})_2$ complex dissociates in the presence of $ExsE_C$, and that $ExsE_C$ forms a complex with $ExsC_{His6}$.

Lastly, we tested whether a 2-fold molar excess of $ExsD_{His6}$ could dissociate the $(ExsC_{His6\text{-}short})_2$·ExsE complex by co-incubation overnight. The elution profile consisted of two peaks corresponding to $(ExsD_{His6})_2$ and the $(ExsC_{His6\text{-}short})_2$·ExsE complex. The absence a peaks corresponding to free ExsE or the $(ExsD_{His6})$·$(ExsC_{His6\text{-}short})_2$ complex suggests that $ExsD_{His6}$ cannot competitively remove $ExsC_{His6\text{-}short}$ from the $(ExsC_{His6\text{-}short})_2$·ExsE complex under the conditions tested (Fig. 4*C*). Taken together, these experiments demonstrate that the binding affinity of ExsC is stronger for ExsE when compared with that of ExsD.

DISCUSSION

The transcriptional activity of ExsA is controlled through a regulatory cascade consisting of ExsD, ExsC, and ExsE. ExsC is a key player in this regulatory cascade, as it forms a complex with either ExsE or ExsD. Binding of ExsC to ExsE prevents transcription of T3SS genes, whereas binding to ExsD leads to activation of T3SS gene transcription. Here we report that the native states of purified ExsC, ExsD, and ExsE are, respectively, dimeric, trimeric, and monomeric. Our ITC data indicate that the stoichiometry within the ExsC-ExsD complex is 1:1, and the molecular weight of the complex derived from AUC is consistent with a heterotetrameric complex of $ExsC_2$·$ExsD_2$. Similarly, both ITC and AUC data are in agreement that the binding ratio within the ExsC-ExsE complex is 2:1 and that the complex is a

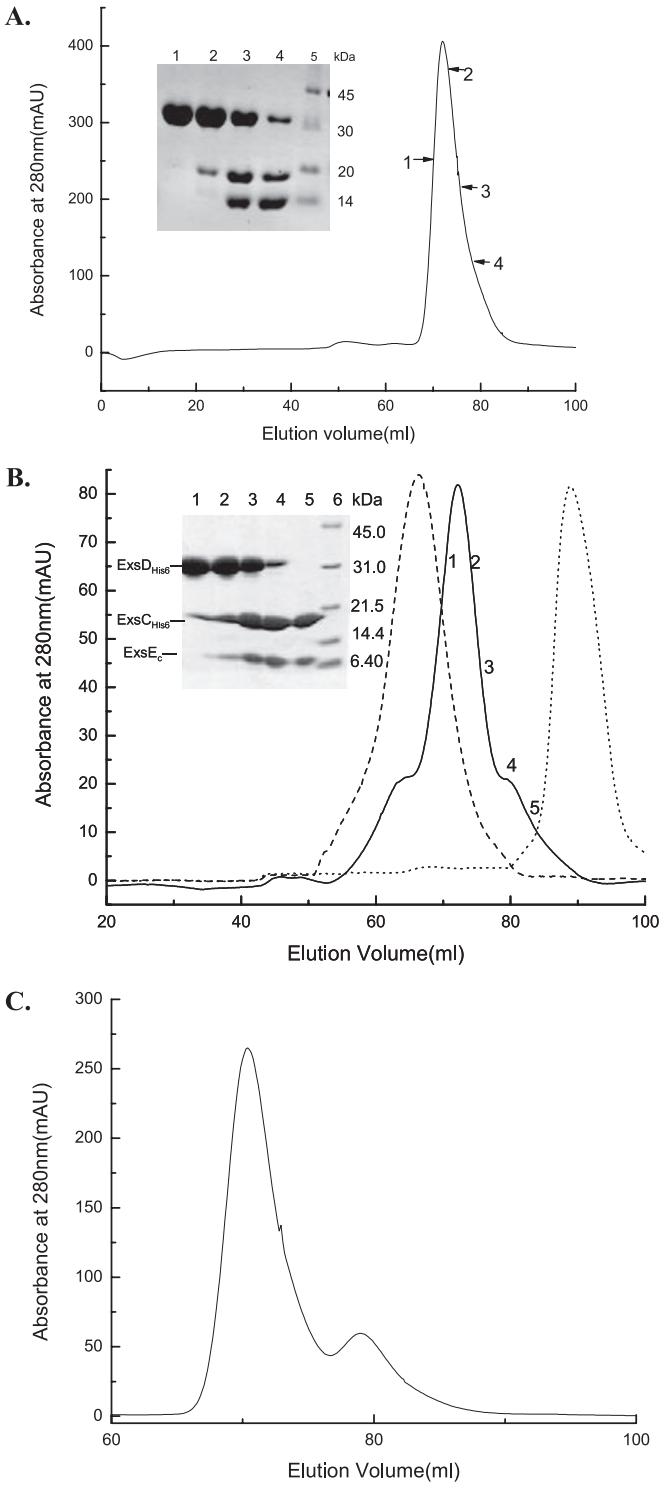

FIGURE 4. **Competitive binding of ExsC to ExsE and ExsD.** *A*, $ExsC_{His6}$, $ExsD_{His6}$, and $ExsE_C$ were mixed at a 1:1:0.5 molar ratio and incubated at 4 °C overnight. The resulting asymmetric elution peak is the overlap of $ExsD_{His6}$ (71.4 ml, which has a broad profile) and $ExsC_{His6}$-$ExsE_C$ (74.7 ml). The compositions of representative fractions before (fraction *1*) and after the peak position (fractions *2–4*) were resolved by SDS-PAGE as shown in the *insert*. *B*, $ExsE_C$ was incubated with purified $ExsC_{His6}$-$ExsD_{His6}$ (*solid line*) at a 2:1 molar ratio at 4 °C overnight. The elution profiles of the $ExsC_{His6}$-$ExsD_{His6}$ complex (centered at 66.4 ml, *dashed line*) and $ExsE_C$ (centered at 88.8 ml, *dotted line*) are included for reference. The compositions of representative fractions were examined by SDS-PAGE as shown in the *insert*. *C*, $ExsD_{His6}$ was added into the purified $ExsC_{His6\text{-}short}$-ExsE complex at a 2:1 molar ratio and incubated at 4 °C overnight. No new molecular species was formed, given that the two elution peaks correspond to the input samples: $ExsC_{His6\text{-}short}$-ExsE, 79.5 ml; $ExsD_{His6}$, 71.4 ml.

heterotrimer of $ExsC_2$·ExsE. Affinity measurements and binding studies show that ExsC binds ExsE stronger than ExsD, supporting a model in which the preferential binding of ExsC to ExsE favors formation of the transcriptionally inactive ExsD-ExsA complex.

Although the carboxyl-terminal tags used for purification of ExsC, ExsD, and ExsE did not affect self-association or complex formation, they did substantially increase the hydrodynamic volume of the proteins (as reflected by the decrease in the elution volume during gel filtration chromatography). For example, the carboxyl-terminal tags in the $(ExsC_{His6})_2$·$ExsE_C$ complex add an additional 4.4 kDa of mass relative to the $(ExsC_{His6\text{-}short})_2$·ExsE complex. This additional 4.4 kDa resulted in a drastic increase in the apparent molecular mass as estimated by gel filtration (63.4 kDa for the $(ExsC_{His6\text{-}short})_2$·ExsE complex when compared with 96.1 kDa for the $(ExsC_{His6})_2$·$ExsE_C$ complex). Similarly, the additional 10.1 kDa of mass in the $(ExsC_{His6})_2$·$(ExsD_{His6})_2$ complex when compared with the $(ExsC_{His6\text{-}short})_2$·$ExsD_2$ complex results in an increase of 35.7 kDa in the molecular mass estimated by gel filtration (197.5 kDa for $(ExsC_{His6})_2$·$(ExsD_{His6})_2$ compared with 161.8 kDa for the $(ExsC_{His6\text{-}short})_2$·$ExsD_2$ complex). In deriving the apparent molecular mass by gel filtration, a compact globular shape is assumed, and globular proteins are used in the standard calibration. For macromolecules with asymmetric shapes, the apparent molecular mass values from gel filtration tend to be significantly overestimated (18). Thus, the drastic increase in the hydrodynamic volume due to the presence of the carboxyl-terminal tag indicates that these extensions are highly flexible and contribute significantly to the asymmetric shape of the fusion proteins. In contrast to the gel filtration method, the molecular mass values derived from equilibrium sedimentation analytical ultracentrifugation do not rely on model presumption (19); therefore, AUC is an accurate technique to use in assessing the association states of self-associated and in complex. Within the experimental errors, AUC-derived molecular mass values of $(ExsC_{His6})_2$·$ExsE_C$ and $(ExsC_{His6\text{-}short})_2$·ExsE (46.9 ± 1.2 kDa and 45.7 ± 1.0 kDa, respectively) better reflect the predicted difference of 4.4 kDa and are in good agreements with their respective theoretical values.

Members of the class I family of type III secretion chaperones, including SycE, SigE, SicP, and CesT (13), are homodimers, and the largely hydrophobic dimeric interface is extensive (20, 21), suggesting a strong dimer association. In line with this structural observation, subunit dissociation of the dimeric ExsC reported in this study is minimal. Another structural feature conserved in these secretion chaperones is the exposure of hydrophobic patches on the surface of the homodimer. These hydrophobic regions have been implicated in the interaction with the secreted substrate, and the hydrophobic interaction has been further shown to be the major contributing factor to the energy release resulting from complex formation (20, 22). Our observation that a large enthalpy ($\Delta H = -31.5$ kcal/mol, from ITC experiments) is released accompanying the ExsC-ExsE complex formation supports the idea that the interaction between ExsC and ExsE is also mainly hydrophobic. Like other secretion chaperones (20), the dimeric struc-

ture of ExsC is very likely unaffected upon forming the complex with the secreted substrate ExsE.

The proposed functions of secretion chaperones include protecting the substrate from degradation, preventing the substrate from aggregation or premature interaction with downstream components, maintaining the substrate in a secretion-competent state, and together with the substrate forming a targeting motif for secretion (23). In *Salmonella typhimurium*, the type III secretion chaperone SicP is required to stabilize the structure of its substrate SptP. In the absence of SicP mutant, the degradation rate of SptP is elevated (24). Similarly, ExsC has been shown to stabilize ExsE and increase the efficiency of ExsE secretion (10). Although highly soluble, ExsE does not adopt substantial secondary or tertiary structure as suggested by circular dichroism (CD) and nuclear magnetic resonance (NMR) studies.[3] The lack of structural elements suggests that ExsE exists as an assembly of various conformations, *i.e.* that its structure is highly dynamic. It is conceivable that only certain conformations are compatible for binding ExsC. For ExsE, loss of conformational freedom because of complex formation with ExsC may account for the overall entropy decrease measured by ITC ($ExsC_2 + ExsE \rightarrow ExsC_2{\cdot}ExsE$, $\Delta S = -64.7$ cal/mol). In comparison, the entropy change is favorable for ExsC·ExsD complex formation ($ExsC_2 + ExsD_3 \rightarrow ExsC_2{\cdot}ExsD_2$, $\Delta S = +11.3$ cal/mol). The unfavorable entropic decrease in forming the ExsC-ExsE complex is overcome by the large amount of enthalpic release, as discussed above, such that the overall complex formation is thermodynamic favorable ($\Delta G < 0$). Our data thus far support a model in which by assisting ExsE in adopting certain conformations, ExsC confers structural stability to ExsE and may possibly prime ExsE for secretion.

Besides interacting with ExsE as a secretion chaperone, ExsC also forms complex with the anti-activator ExsD to regulate T3SS gene transcription (9). Our observation of dynamic interaction between subunits in the trimeric ExsD supports a mechanism for ExsC-ExsD complex formation in which one monomer dissociates from the trimeric ExsD, whereas the other two monomers may be rearranged to accommodate the dimeric ExsC. The enthalpy release during this complex formation is modest (7.6 kcal/mol) compared with that of ExsC-ExsE formation, suggesting that the interaction in ExsC-ExsD complex is unlike that in ExsC-ExsE, which is largely hydrophobic. The difference in the nature of these interactions (as reflected by the difference in enthalpy change) suggests that ExsD and ExsE may bind to discrete regions of ExsC. Ultimately, determining the binding sites of ExsD and ExsE on ExsC, as well as the interplay between ExsC and ExsD or ExsC and ExsE, will await structural determination of the ExsD-ExsC and ExsC-ExsE complexes.

[3] Z. Zheng, E. D. Brutinel, T. L. Yahr, and L. Chen, unpublished results.

Acknowledgments—We thank V. Fiscus, E. Daniel, and M. Afrane for assistance with the protein purification and T. Stone for AUC and ITC measurements.

REFERENCES

1. Richards, M. J., Edwards, J. R., Culver, D. H., and Gaynes, R. P. (1999) *Crit. Care Med.* **27,** 887–892
2. Richards, M. J., Edwards, J. R., Culver, D. H., and Gaynes, R. P. (2000) *Infect. Control Hosp. Epidemiol.* **21,** 510–515
3. Barbieri, J. T., and Sun, J. (2004) *Rev. Physiol. Biochem. Pharmacol.* **152,** 79–92
4. Sato, H., and Frank, D. W. (2004) *Mol. Microbiol.* **53,** 1279–1290
5. Frank, D. W., and Iglewski, B. H. (1991) *J. Bacteriol.* **173,** 6460–6468
6. Vallis, A. J., Yahr, T. L., Barbieri, J. T., and Frank, D. W. (1999) *Infect. Immun.* **67,** 914–920
7. Frank, D. W. (1997) *Mol. Microbiol.* **26,** 621–629
8. McCaw, M. L., Lykken, G. L., Singh, P. K., and Yahr, T. L. (2002) *Mol. Microbiol.* **46,** 1123–1133
9. Dasgupta, N., Lykken, G. L., Wolfgang, M. C., and Yahr, T. L. (2004) *Mol. Microbiol.* **53,** 297–308
10. Urbanowski, M. L., Lykken, G. L., and Yahr, T. L. (2005) *Proc. Natl. Acad. Sci. U. S. A.* **102,** 9930–9935
11. Rietsch, A., Vallet-Gely, I., Dove, S. L., and Mekalanos, J. J. (2005) *Proc. Natl. Acad. Sci. U. S. A.* **102,** 8006–8011
12. Feldman, M. F., and Cornelis, G. R. (2003) *FEMS Microbiol. Lett.* **219,** 151–158
13. Page, A. L., and Parsot, C. (2002) *Mol. Microbiol.* **46,** 1–11
14. Parsot, C., Ageron, E., Penno, C., Mavris, M., Jamoussi, K., d'Hauteville, H., Sansonetti, P., and Demers, B. (2005) *Mol. Microbiol.* **56,** 1627–1635
15. Wei, C. F., Deng, W. L., and Huang, H. C. (2005) *Mol. Microbiol.* **57,** 520–536
16. Walker, K. A., and Miller, V. L. (2004) *J. Bacteriol.* **186,** 4056–4066
17. Lykken, G. L., Chen, G., Brutinel, E. D., Chen, L., and Yahr, T. L. (2006) *J. Bacteriol.* **188,** 6832–6840
18. le Maire, M., Viel, A., and Moller, J. V. (1989) *Anal. Biochem.* **177,** 50–56
19. van Holde, K. E., Johnson, W. C., and Ho, P. S. (eds) (1998) in *Principles of Physical Biochemistry*, pp. 194–212, Prentice Hall, Upper Saddle River, NJ
20. Birtalan, S., and Ghosh, P. (2001) *Nat. Struct. Biol.* **8,** 974–978
21. Luo, Y., Bertero, M. G., Frey, E. A., Pfuetzner, R. A., Wenk, M. R., Creagh, L., Marcus, S. L., Lim, D., Sicheri, F., Kay, C., Haynes, C., Finlay, B. B., and Strynadka, N. C. (2001) *Nat. Struct. Biol.* **8,** 1031–1036
22. Birtalan, S. C., Phillips, R. M., and Ghosh, P. (2002) *Mol. Cell* **9,** 971–980
23. Ghosh, P. (2004) *Microbiol. Mol. Biol. Rev.* **68,** 771–795
24. Fu, Y., and Galan, J. E. (1998) *J. Bacteriol.* **180,** 3393–3399